Bull. Chem. Soc. Ethiop. **2025**, 39(6), 1095-1108.
DOI: https://dx.doi.org/10.4314/bcse.v39i6.6

ISSN 1011-3924
Printed in Ethiopia
Online ISSN 1726-801X

SYNTHESIS, SPECTOSCOPIC, THERMAL, AND MOPHOLOGICAL STUDIES OF METAL-BASED COMPLEXES DERIVED FROM THE REACTION OF CINCHONINE WITH MANGANESE(II), NICKEL(II), AND ZINC(II) IONS

Moamen S. Refat[1*], Abdel Majid A. Adam[1], Q. Mohsen[1] and Amnah Mohammed Alsuhaibani[2]

[1]Department of Chemistry, College of Science, Taif University, P.O. Box 11099, Taif 21944, Saudi Arabia
[2]Department of Sports Health, College of Sport Sciences & Physical Activity, Princess Nourah bint Abdulrahman University, PO Box 84428, Riyadh 11671, Saudi Arabia

(Received January 14, 2025; Revised February 18, 2025; Accepted February 21, 2025)

ABSTRACT. This work involved the meticulous synthesis of three metal-based complexes of the naturally occurring compound cinchonine (abbreviated as CN), which belongs to the *Cinchona* alkaloids family and exhibits potent antimalarial properties. Studying these metal-based complexes is crucial, as it enhances our understanding of cinchonine's biological characteristics. The CN complexes were carefully prepared by dissolving the CN ligand in methanol and the investigated Mn(II), Ni(II), and Zn(II) metal ions in deionized water. The chemical reactions were carried out at a controlled temperature of 70 °C, a 1:1 (CN to metal ion) stoichiometry, and a pH of approximately 8.5. These conditions yielded the desired CN-Mn, CN-Ni, and CN-Zn complexes, which were subsequently characterized using various physicochemical techniques. The comprehensive characterization provided detailed insights into the structural, thermal, and morphological properties of the complexes. The results indicate that the CN complexes with Mn(II), Ni(II), and Zn(II) can be represented by the formulas $[MnCN(H_2O)_3Cl_2]$, $[NiCN(H_2O)_5]\cdot Cl_2\cdot 2H_2O$, and $[ZnCN(H_2O)_5]\cdot Cl_2\cdot 4H_2O$, respectively. The IR spectral data suggests that the CN ligand coordinated with the Mn(II), Ni(II), and Zn(II) ions through the nitrogen lone pair electrons of the C=N group. The high-quality and well-focused TEM images demonstrate the complexes possessed a uniform and well-structured morphology.

KEY WORDS: Cinchonine, Metal ions, Spectroscopic analyses, Thermal characterization, Electron microscopy

INTRODUCTION

Metal complexes are chemical compounds formed by the reaction of metals with specific molecules called ligands. These complexes are crucial in life-saving research. The metal coordinates with the ligands through covalent bonds. The ligands, like Lewis bases, donate electron pairs, and the metals, like Lewis acids, accept them. Ligands can be organic or inorganic, neutral, cationic, or anionic, and have one or more electron pairs to share with metals. They can be categorized as monodentate, bidentate, tridentate, or polydentate based on the number of donating atoms. Metal complexes have unique properties like spectroscopic, photophysical, electrochemical, and biological activities, including antioxidant, chemotherapeutic, and antimicrobial effects. These properties have life-saving potential in diverse fields like materials science, medicine, and catalysis [1-9]. Transition metals are vital in designing metal-based drugs for conditions like cancer, neurological disorders, infections, and diabetes [10, 11]. Metal complexes also play a role in disease diagnosis. Researchers are increasingly interested in producing, analyzing, and using metal-based complexes, which are essential for studying interactions between bioactive molecules and metal ions, crucial for developing innovative metallodrugs [12-21].

*Corresponding authors. E-mail: msrefat@tu.edu.sa

Cinchonine (CN), a member of the *Cinchona* alkaloids family, is a naturally occurring compound with potent antimalarial abilities. Originally, cinchonine was commonly extracted from the bark of *Cinchona officinalis* trees native to South America [22]. The bark of these *Cinchona* trees and shrubs found in Bolivia, Ecuador, and Peru has long served as an effective remedy against malaria, for over 400 years. Its use in Europe dates back to the 17th century. Quinine (QN), the active ingredient, was first isolated in 1820 by Pelletier and Caventou. This discovery led to improved efficiency of antimalarial treatment by replacing the bark with its unknown alkaloid content with purified quinine (QN). Quantification methods also allowed botanists to selectively cultivate *Cinchona* varieties rich in these alkaloids. Currently, a few alkaloids are produced on an industrial scale, including the four major ones found in *Cinchona officinalis* bark: cinchonine (CN), cinchonidine (CD), quinidine (QD), and quinine (QN) [23]. *Cinchona* alkaloids consist of three largely independent components: a central hydroxyl group, a bulky bicyclic quinuclidine moiety with a vinyl substituent, and an aromatic quinoline ring. The aromatic quinoline moiety is responsible for the antimalarial properties of *Cinchona* alkaloids. Malaria is a tropical disease caused by a protozoan parasite transmitted by Anopheles mosquitoes. *Cinchona* alkaloids have been widely used as antimalarial drugs for centuries, and their discovery and isolation have played a crucial role in the treatment of this devastating disease [24].

This study examines the complexation characteristics of cinchonine (abbreviated as CN), with three metal ions (i.e., Mn(II), Ni(II), and Zn(II)). The CN ligand reacted with the selected metal ions under specific conditions: a 1:1 stoichiometric ratio, a reaction temperature of 70 °C, and a pH of approximately 8.5. The resulting metal-based complexes were isolated, purified, and then analyzed using various physicochemical techniques, including ultraviolet/visible (UV-Visible), Fourier-transform infrared (FT-IR), powder X-ray diffraction (XRD), and thermogravimetry analyses. Spectral, elemental, and thermal data were obtained to characterize the complexes. Finally, the morphology of the complexes was observed using transmission electron microscopy (TEM) to gain insight into their structural properties.

EXPERIMENTAL

Materials

The investigated metal ions were in type of chloride salts purchased from Merck Chemical Company (KGaA, Germany). These included manganese(II) chloride ($MnCl_2$; 125.84 g/mol; purity ≥ 99%), nickel(II) chloride ($NiCl_2$; 129.60 g/mol; purity 98%), and zinc chloride ($ZnCl_2$; 136.30 g/mol; purity 98%). Sigma-Aldrich (St Louis, MO, USA) provided high-purity Cinchonine monohydrochloride ($C_{19}H_{22}N_2O{\cdot}HCl$; 330.85 g/mol; 99%) and HPLC-grade methanol.

Synthesis of CN complexes

Metal-based complexes containing Mn(II), Ni(II), and Zn(II) ions with CN ligand were synthesized through a three-step procedure. First, three portions of methanolic solutions of the CN ligand were prepared by dissolving 3 mmol of CN in 30 mL of methanol. Next, these CN solutions were gradually added to aqueous solutions of Mn(II), Ni(II), and Zn(II) ions, each containing 3 mmol in 30 mL of deionized water. The resulting CN-Mn, CN-Ni, and CN-Zn mixtures were placed on a hot plate with a magnetic stirrer. In the final step, the mixtures were stirred at 70 °C, and the pH was adjusted to approximately 8.5 using a few drops of 5% ammonia solution. After 20 min of stirring, colored precipitates began to form in each beaker. The beakers were left overnight to ensure complete precipitation of the CN-Mn, CN-Ni, and CN-Zn complexes. The generated metal-based complexes were collected by filtration and purified by washing with hot deionized water, diethyl ether, and methanol. Finally, the CN complexes were

oven-dried at 75 °C and stored in a vacuum desiccator. The metal-based complex of CN obtained using Mn(II) ions was termed the CN-Mn complex, while the one obtained using Ni(II) ions was termed the CN-Ni complex, and the last one was termed the CN-Zn complex.

Characterization techniques

Several physicochemical techniques were employed to comprehensively characterize the metal-based complexes in terms of their structural, thermal, and morphological properties. Spectral analyses of the complexes were conducted using a Cary 7000 Agilent Technologies UV-Vis Spectrophotometer, a Bruker ALPHA FT-IR Spectrometer, and a Bruker D8 Advance X-Ray Diffractometer. These analytical tools provided the UV-Vis spectra (200-800 nm), FT-IR spectra (400-4000 cm^{-1}), and XRD patterns (10º-80º), respectively. Additionally, elemental and conductivity measurements were performed using a Perkin-Elmer 2400 series II CHNS analyzer to determine the hydrogen, carbon, and nitrogen contents, and a JENWAY conductivity meter model 4510 to obtain the molar conductance values. Thermal characterizations of the complexes were carried out using a Q500 V20.10 Build 36 Thermal Analyzer, generating the TG/DTG thermograms in the 25-800 °C range under air atmosphere. Finally, transmission electron microscope (TEM) imaging was conducted using a high-resolution JEM-2010 JEOL Microscope at a 200 kV accelerating voltage. The comprehensive characterization of the metal-based complexes using these advanced physicochemical techniques provided a detailed understanding of their structural, thermal, and morphological properties.

RESULTS AND DISCUSSION

UV-Visible spectral data and molar conductance measurements

The DMSO solutions of the free CN ligand and its complexes with Mn(II), Ni(II), and Zn(II) ions were analyzed using a UV-Visible spectrometer, and the resulting spectra are presented in Figure 1. The uncomplexed CN ligand exhibits a limited absorption profile, absorbing light from 200 to 400 nm. The UV-Visible spectrum of the free ligand is characterized by a very strong, broad absorption band centered at 304 nm, with a width of approximately 100 nm. Additionally, the spectrum includes a weak absorption band at 200 nm, both of which can be attributed to $\pi \rightarrow \pi^*$ transitions. The characteristic 304 nm absorption band is still observed in the CN-Ni and CN-Zn complexes, albeit with a slight decrease in intensity. In the CN-Mn complex, this band is significantly reduced in intensity and red-shifted to 327 nm. The spectra of the CN-Mn, CN-Ni, and CN-Zn complexes all contain a weak absorption band around 200 nm, with the same intensity, width, and position as in the free CN ligand. The CN-Ni complex also displays two additional absorption bands at 440 and 688 nm. The observed spectral changes upon the reaction of the free CN ligand with Mn(II), Ni(II), and Zn(II) metal ions can be attributed to the complexation process and potential metal-to-CN ligand charge transfer (MLCT) transitions. The UV-Visible profiles of the CN-Mn, CN-Ni, and CN-Zn complexes suggest that the coordination of the Mn(II), Ni(II), and Zn(II) metal ions to the CN ligand has a significant impact on the electronic structure and optical properties of the resulting complexes. These findings provide valuable insights into the interactions between the CN ligand and the investigated metal ions, which can have important implications for the design and development of new coordination complexes with tailored optical and electronic properties.

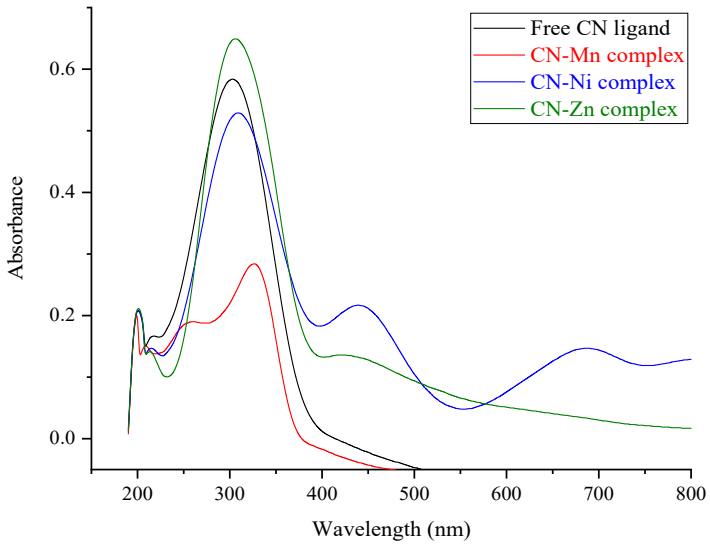

Figure 1. UV-Visible spectra of free CN ligand, CN-Mn, CN-Ni, and CN-Zn complex.

The molar conductance of the free CN ligand, as well as the CN-Mn, CN-Ni, and CN-Zn complexes, was measured using a JENWAY conductivity meter model 4510. These four compounds were dissolved in DMSO solvent at a concentration of 10^{-3} M, and their conductivity values were found to be 7.24, 32.94, 142.68, and 180.72 S cm^2 mol^{-1} for the free CN ligand, CN-Mn, CN-Ni, and CN-Zn complex, respectively. The DMSO solution of the free ligand exhibits non-conductive behavior, while the ligand's complexes demonstrate electrolytic properties. The non-conductive nature of the free CN ligand and the electrolytic behavior of the CN-Mn, CN-Ni, and CN-Zn complexes can be attributed to the presence of chloride ions within the structure of the complexes. The high conductivity of the CN-Ni and CN-Zn complexes suggests a substantial number of chloride ions in their structures, indicating a higher degree of ionic character in these complexes compared to the CN-Mn complex.

Elemental composition analysis

Metal-based complexes containing a CN ligand were prepared by dissolving the ligand in methanol and dissolving the investigated metal ions in deionized water. The chemical reaction was carried out by controlling the temperature at 70 °C, the stoichiometry at 1:1 (CN to metal ion), and the pH at approximately 8.5. Under these conditions, the reactions yielded the desired CN-Mn, CN-Ni, and CN-Zn complexes, which have been found to be soluble in N,N-dimethylformamide (DMF) and dimethyl sulfoxide (DMSO) solvents, but insoluble in water and most organic solvents. The elemental composition of the manufactured complexes was analyzed using an elemental analyzer to determine the content of C, N, Cl, and H elements, and gravimetric analysis was used to determine the metal (Mn, Ni, Zn) and water content. Table 1 summarizes the percentage composition of carbon, nitrogen, chlorine, hydrogen, metal, and water in the CN-Mn, CN-Ni, and CN-Zn complexes. The results presented in Table 1 provide valuable insights into the stoichiometry and purity of the synthesized complexes, which is crucial for understanding their

chemical and physical characteristics. The experimental percentages of C, N, Cl, H, metal, and water closely match the calculated values, confirming the accuracy of the analysis. The composition data suggests a 1:1 (metal to CN ligand) stoichiometry between the CN ligand and the investigated metal ions. The elemental analysis indicates that the CN complexes with Mn(II), Ni(II), and Zn(II) can be represented by the formulas $[MnCN(H_2O)_3Cl_2]$, $[NiCN(H_2O)_5]\cdot Cl_2\cdot 2H_2O$, and $[ZnCN(H_2O)_5]\cdot Cl_2\cdot 4H_2O$, respectively. The overall compositions for the proposed formulas $C_{19}H_{28}N_2Cl_2O_4Mn$, $C_{19}H_{36}N_2Cl_2O_8Ni$, and $C_{19}H_{40}N_2Cl_2O_{10}Zn$ correspond to the CN-Mn, CN-Ni, and CN-Zr complexes, respectively. The calculated molecular weights for these proposed formulas are 443.60 g/mol, 549.98 g/mol, and 592.67 g/mol, respectively. These findings provide valuable insights into the stoichiometry and purity of the synthesized complexes, which are crucial for understanding their chemical and physical properties.

Table 1. The percentage composition (%) of C, N, Cl, H, metal, and water in the manufactured CN-Mn, CN-Ni, and CN-Zn complexes.

Complex	Results											
	Found (%)						Calculated (%)					
	C	H	Cl	N	Metal	H_2O	C	H	Cl	N	Metal	H_2O
Mn(II)	51.18	6.43	16.12	6.50	5.36	12.00	51.40	6.31	15.98	6.31	5.48	12.17
Ni(II)	41.28	6.80	12.73	5.27	10.52	22.66	41.46	6.55	12.89	5.09	10.67	22.90
Zn(II)	38.60	6.62	12.19	4.95	11.19	27.20	38.47	6.75	11.96	4.72	11.03	27.33

FT-IR spectral data

The infrared spectral data can be used to predict the coordination site in the CN ligand that participates in the formation of metal-based complexes. This can be accomplished by comparing the differences between the FT-IR spectra of the CN-Mn, CN-Ni, and CN-Zn complexes and the spectrum of the free CN ligand. The experimental FT-IR spectra of the free CN ligand and its complexes with Mn(II), Ni(II), and Zn(II) ions are presented in Figure 2. Comparing the key characteristic IR spectral bands of the free CN ligand with the corresponding bands in the IR spectra of the complexes reveals several changes in the positions and intensities of some of the key bands of the free ligand. These shifts are attributed to the modifications in the electronic structure of the CN unit within the generated complexes relative to the free CN ligand. The CN molecule contains a secondary hydroxyl group (C-OH), which contributes to several absorption bands observed in the IR spectrum of the free CN ligand. The band at 3345 cm^{-1} could be attributed to the stretching υ(-OH) vibrations, while the band at 1323 cm^{-1} can be attributed to the deformation υ(-OH) vibrations. Additionally, the CN molecule contains quinuclidine and quinoline rings, which are responsible for the absorption bands at 3139, 2929, and 2809 cm^{-1}, attributed to the stretching υ(C-H) modes of aryl and alkyl C-H bonds. The CN molecule also exhibits both alkene and aromatic C=C bonds, with the alkene stretching υ(C=C) vibrations resonating at 1591 cm^{-1} and the aromatic stretching υ(C=C) vibrations at 1508 cm^{-1}. The band at 1458 cm^{-1} could be assigned to the stretching υ(C=N) vibrations of the quinoline ring. Furthermore, the alkyl C-H deformation motions are responsible for bands at approximately 1424 and 1389 cm^{-1}. The bands at 1285, 1116, and 1098 cm^{-1} were likely associated with the stretching υ(C–O), υ_{as}(C–N), and υ_{s}(C–N) vibrations, respectively. These interpretations of the CN principal IR bands are consistent with the literature [25-28].

When the CN ligand interacted with the Mn(II), Ni(II), Zn(II) ions, several of the characteristic absorption bands of the CN ligand remained unchanged or were slightly shifted. These bands originated from the υ(-OH), υ(-OH), υ(C–O), υ_{as}(C–N), and υ_{s}(C–N) vibrations. Specifically, in the IR spectrum of the CN-Mn complexes, these bands were observed at 3349, 1319, 1284, 1115,

and 1099 cm^{-1}, respectively. For the CN-Ni complex, the bands appeared at 3345, 1321, 1283, 1116, and 1095 cm^{-1}, respectively. The corresponding frequencies for the CN-Zn complex were 3347, 1326, 1287, 1111, and 1099 cm^{-1}, respectively. The band originated from the υ(C=N) vibrations was significantly shifted in the corresponding metal-based complexes. This band was observed at 1458 cm^{-1} in the free CN ligand, but it shifted to 1425 cm^{-1} in the CN-Mn complex, 1427 cm^{-1} in the CN-Ni complex, and 1430 cm^{-1} in the CN-Zn complex. The IR spectra of CN-Mn, CN-Ni, and CN-Zn complexes also contained new medium-intensity absorption bands at 580, 583, and 575 cm^{-1}, respectively [29]. These bands could be assigned to the stretching vibrations of Mn–N, Ni–N, and Zn–N bonds, respectively. The IR spectral data suggested that the CN ligand coordinated with the Mn(II), Ni(II), and Zn(II) through the nitrogen lone pair electrons of the C=N group. The coordinated water molecules in the complexes were responsible for the absorption bands found in the region 1640-1630, 865-840, 670-665, and 585-580 cm^{-1}, which can be attributed to the $\delta_{bend}(H_2O)$, $\delta_{rock}(H_2O)$, $\delta_{wag}(H_2O)$, and $\delta_{twist}(H_2O)$, respectively [30]. The collected elemental, conductivity, and spectral data were used to propose the chemical structure of the synthesized CN-Mn, CN-Ni, and CN-Zn complexes, as depicted in Figure 3.

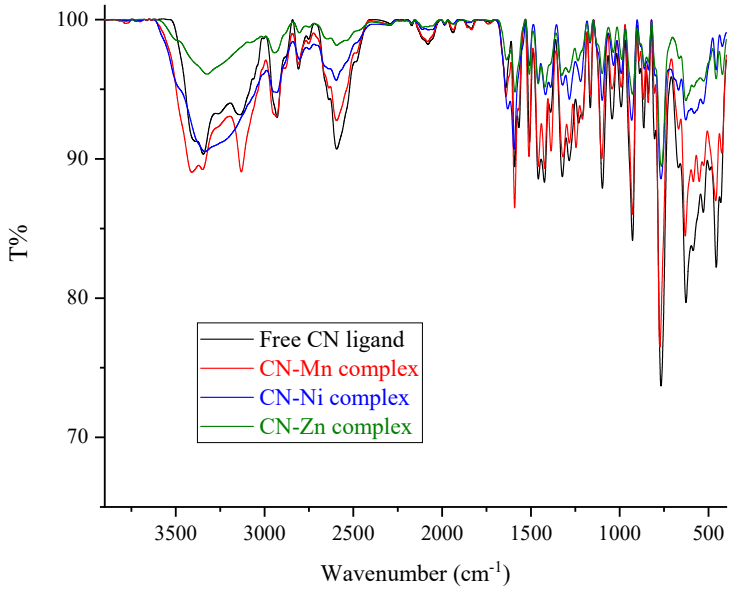

Figure 2. FT-IR spectra of free CN ligand, CN-Mn, CN-Ni, and CN-Zn complex.

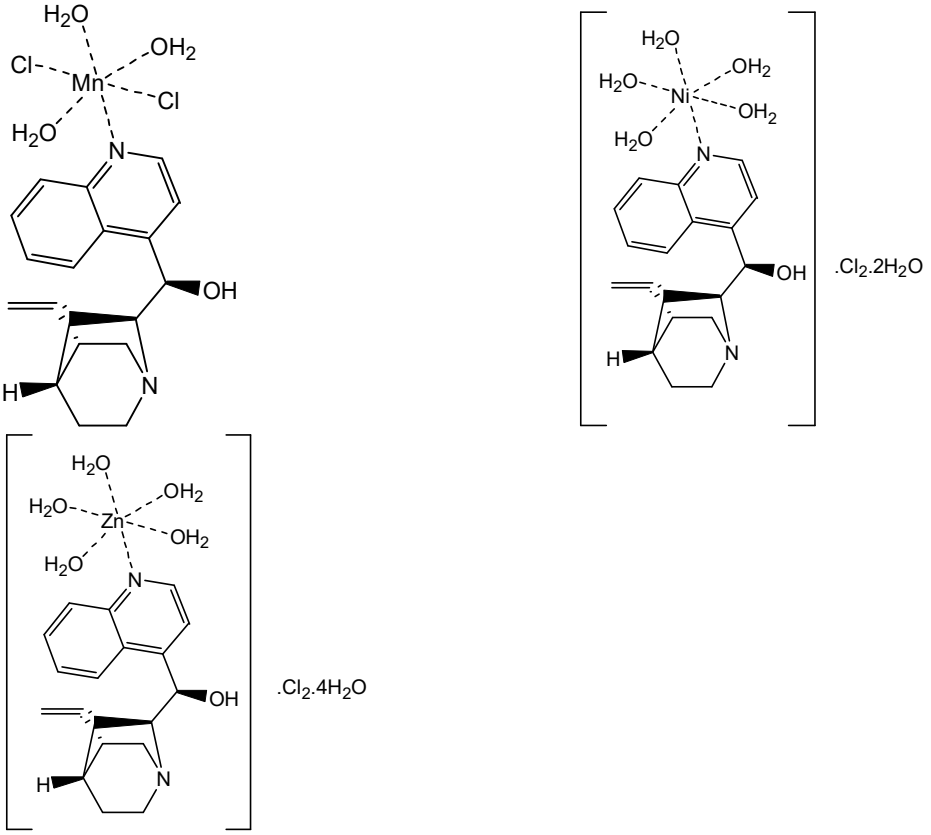

Figure 3. The suggested chemical structures of the synthesized complexes.

Powder X-ray diffraction profiles and TEM imaging

A Bruker D8 Advance X-Ray Diffractometer was used to record the powder X-ray diffraction profiles of the free CN ligand and its metal-based complexes. The XRD patterns were analyzed to determine the framework structure and phase purity of the CN-Mn, CN-Ni, and CN-Zn complexes. The XRD instrument employed a Cu $K_{\alpha 1}$ source, a Ge monochromator, a wavelength of 0.154056 nm, and operating parameters of 40 kV and 30 mA. The powdered samples were scanned from a diffraction angle (2θ) of 10° to 70° at 25 °C. The XRD analysis of the free CN ligand revealed five diffraction lines, including one very strong line and four medium-intensity lines. The strongest line was observed at a 2θ Bragg's angle of 17.269°, while the four medium-intensity diffraction lines were located at 2θ values of 10.453°, 19.110°, 21.267°, and 24.59°. The XRD diffractogram of the CN-Mn complex exhibited seven characteristic reflections: a very strong line at 2θ 19.418°, two medium-strong diffraction patterns at 2θ 8.793° and 14.633°, and four medium-intensity lines at 2θ 12.575°, 13.796°, 17.735°, and 20.298°. The XRD profile of the CN-Zn complex displayed six reflections at 2θ Bragg's angle of 10.202° (very strong), 18.191° (medium), 25.176° (medium), 26.179° (medium), 28.036°(medium), and 42.047°(medium). The most intense diffraction line for the free CN ligand, CN-Mn, CN-Ni, and CN-Zr complexes corresponded to *d*-spacing values of 5.12947 Å, 4.56766 Å, 4.84650 Å, and 8.66380 Å, respectively.

The size and morphology of the particles of the free CN ligand and its metal-based complexes were visualized using a TEM microscope. Figures 4, 5, 6, and 7 present the TEM images of the free CN ligand, the CN-Mn complex, the CN-Ni complex, and the CN-Zn complexes, respectively. The high-quality and well-focused TEM images indicate that most of the CN ligand's particles are spherical and uniformly dispersed, with no accumulation. However, some of the ligand particles lack a defined or complete shape. Most ligand particles exhibit diameters ranging from 100 to 150 nm. When the CN ligand formed a complex with Mn(II) ions, the spherical morphology of the particles transformed into a mix of elliptical and oval shapes. Most of the CN-Mn complex particles have diameters between 250 and 350 nm. The interaction of the ligand with Ni ions resulted in rod-shaped particles. The rods of the CN-Ni complex vary in size and thickness, and some tend to aggregate into larger clusters. The average length of these complex rods is approximately 100-120 nm, with an average width of 30-50 nm. The complexation of the CN ligand with Zn ions also led to rod-like particles. The TEM images of the CN-Zn complex show that the rods of this complex have varying sizes and thicknesses, and they also tend to aggregate into larger clusters. Most rods exhibit lengths ranging from 150 to 300 nm and widths between 60 to 80 nm. The analysis of the size and morphology of these particles provides valuable insights into the structural characteristics of the free CN ligand and its metal-based complexes, which can be important for understanding their physical and chemical properties. The morphology of the synthesized products depends on the metal ion that forms the chemical structure of the complex. Complexes containing Zn(II) and Ni(II) ions generate particles with a rod-like morphology, whereas those containing a Mn(II) ion produce a mixture of elliptical and oval-shaped particles. The specific characteristics of the metal ions, such as their atomic radius, electronegativity, and coordination preferences, play a crucial role in determining the final morphology of the synthesized products.

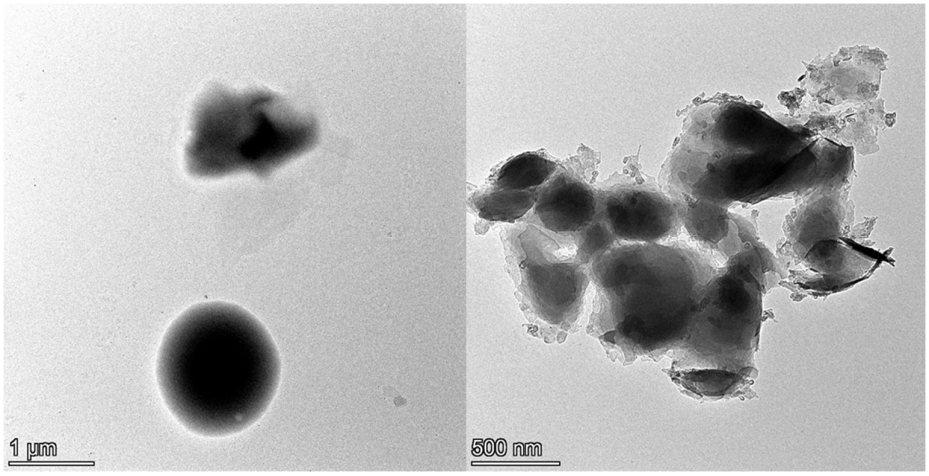

Figure 4. TEM images of the free CN ligand.

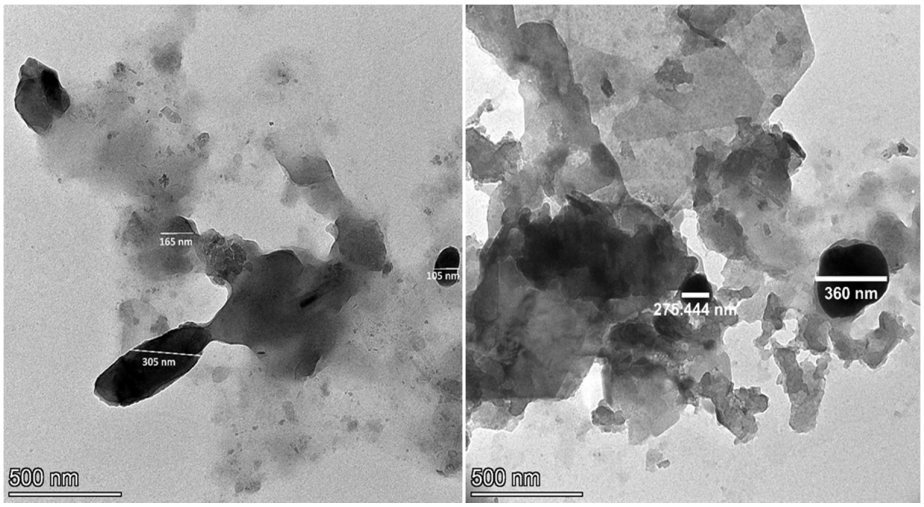

Figure 5. TEM images of the CN-Mn complex.

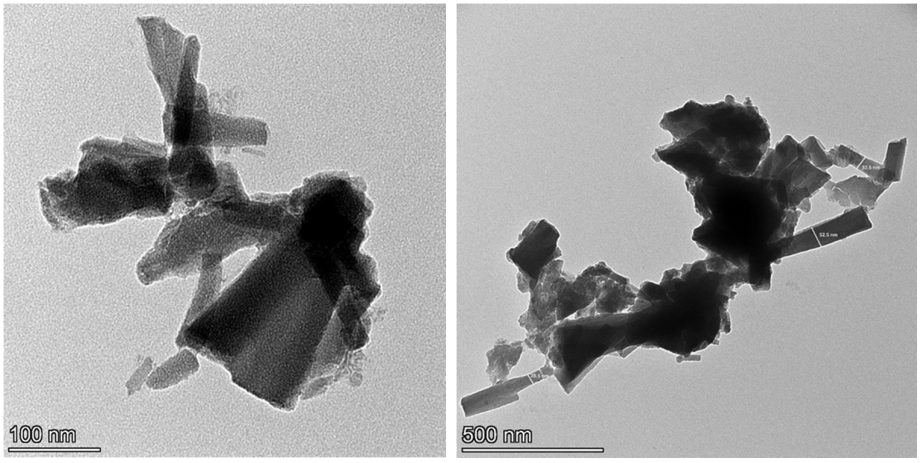

Figure 6. TEM images of the CN-Ni complex.

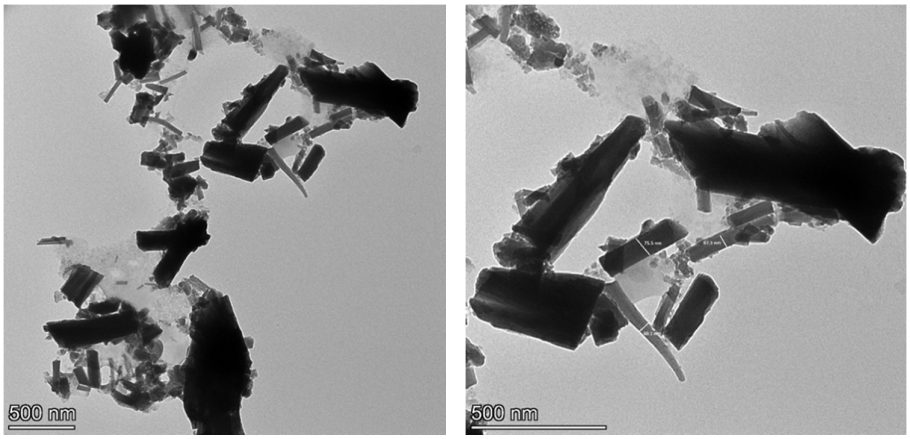

Figure 7. TEM images of the CN-Zn complex.

Thermal decomposition

The thermal decomposition analysis provides insight into the structural characteristics and thermal stability of the synthesized complexes. The thermal decompositions (TG/DTG) of the synthesized CN-Mn, CN-Ni, and CN-Zn complexes were analyzed to verify their proposed compositions and structures of these complexes, which were $[MnCN(H_2O)_3Cl_2]$, $[NiCN(H_2O)_5]\cdot Cl_2\cdot 2H_2O$, and $[ZnCN(H_2O)_5]\cdot Cl_2\cdot 4H_2O$, respectively. These proposed compositions were based on elemental, conductivity, and spectral data, and the thermal analysis confirmed structures. The thermal decomposition data summarized in Table 2, obtained from DG/DTG thermograms of the free CN ligand and its complexes, enabled the following observations: (i) The observed weight losses in each decomposition step matched the expected weight losses for the free CN ligand and its complexes. (ii) The free CN ligand demonstrates thermal stability up to 210 °C, while its complex with Mn(II) exhibits good thermal stability up to 260 °C. In contrast, the complexation of the CN ligand with Ni(II) and Zn(II) ions reduces its thermal stability, with the Ni(II) and Zn(II) complexes starting their thermal decompositions at approximately 100°C and 80°C, respectively. (iii) The thermal stability of the CN metal-based complexes increased in the order CN-Zn < CN-Ni < CN-Mn. This trend is influenced by various factors, including the strength of the metal-ligand bonds, the coordination environment, and the nature of the metal ion. (iv) The complexes of Ni(II) and Zn(II) underwent a three-step degradation process, whereas the Mn(II) complex degraded in a single step. (v) The Ni(II) and Zn(II) complexes exhibited a multi-step degradation process, with the release and thermal decomposition of the CN ligand occurring during the second and third steps. (vi) The thermal decomposition of the complexes resulted in metal oxides as the final residues. The Mn(II) complex produced MnO contaminated with some residual carbons, while the Ni(II) and Zn(II) complexes yielded NiO and ZnO, respectively, without any residual carbons.

The thermograms of the free CN ligand and its complex with Mn(II) ion indicate they exhibit thermal stability up to 210 °C and 260 °C, respectively. Their thermal decompositions occur through a single degradation step, with a DTG_{max} of 296 °C, and 376 °C, respectively. The free ligand's weight loss in this step can be attributed to the release of $9C_2H_2$, N_2, CO, $2H_2$, and HCl molecules (observed; 99.75%, calculated; 100.0%). The weight loss for the CN-Mn complex in this step is due to the loss of $3H_2O$, $8C_2H_2$, N_2, $3H_2$, and Cl_2 molecules (observed; 82.35%,

calculated; 82.71%). The final decomposition product of the CN-Mn complex is manganese(II) oxide (MnO), contaminated with some residual carbon. Thermoanalytical responses of the CN-Ni complex revealed that it decomposed in three distinct stages at DTG_{max} of 188, 293, and 382 ºC. The weight losses associated with these maximum temperatures were 19.52% (calculated; 19.43%), 21.17% (calculated; 21.46%), and 45.30% (calculated; 45.46%), respectively. The complex underwent a three-step degradation process, with each step involving the loss of specific structural components, such as water vapor, gases, organic moieties, and inorganic metal oxide. The three degradation steps of C-Ni complex were assigned to the loss of the ($2H_2O + Cl_2$), ($5H_2O + N_2$), and ($9C_2H_2 + CO + 2H_2$), respectively. The third and final decomposition stage results in NiO as the final product, with no residual carbon remaining. Thermoanalytical responses of the CN-Zn complex revealed that it decomposed in three distinct stages at DTG_{max} of 115, 282, and 411 ºC. The weight losses associated with these maximum temperatures were 23.80% (calculated; 24.11%), 20.00% (calculated; 19.91%), and 41.75% (calculated; 42.18%), respectively. The three degradation steps of C-Zn complex were assigned to the loss of the ($4H_2O + Cl_2$), ($5H_2O + N_2$), and ($9C_2H_2 + CO + 2H_2$), respectively. The third and final decomposition stage culminates in the formation of NiO as the ultimate product, with no leftover carbon present.

Table 2. The potential thermal degradation patterns for the free PC ligand and its metal-based complexes.

Compound	Stages	TG range (°C)	DTG max. (°C)	TG% mass loss		Lost species
				Found	Calculated	
Free CN ligand	I	210-800	296	99.75	100.0	$9C_2H_2 + N_2 + CO + 2H_2$+ HCl
CN-Mn complex	I	260-800	376	82.35	82.71	$3H_2O + 8C_2H_2 + N_2 + 3H_2 + Cl_2$
	Residue	-	-	17.00	17.09	MnO + 3C
CN-Ni complex	I	100-225	188	19.52	19.43	$2H_2O + Cl_2$
	II	225-330	293	21.17	21.46	$5H_2O + N_2$
	III	330-800	382	45.30	45.46	$9C_2H_2 + CO + 2H_2$
	Residue	-	-	13.60	13.58	NiO
CN-Zn complex	I	80-200	115	23.80	24.11	$4H_2O + Cl_2$
	II	200-350	282	20.00	19.91	$5H_2O + N_2$
	III	350-800	411	41.75	42.18	$9C_2H_2 + CO + 2H_2$
	Residue	-	-	13.46	13.73	ZnO

CONCLUSION

This study synthesized three metal-based complexes from the natural compound cinchonine (CN), an antimalarial *Cinchona* alkaloid. Investigating these complexes is crucial to understanding cinchonine's biological properties. The CN complexes were carefully prepared by dissolving the CN ligand in methanol and the Mn(II), Ni(II), and Zn(II) metal ions in water. The reactions were conducted at 70°C, with a 1:1 ratio, and pH ~8.5, yielding the desired CN-Mn, CN-Ni, and CN-Zn complexes. These complexes were then thoroughly characterized using various analytical techniques. The results indicate the complexes have the formulas $[MnCN(H_2O)_3Cl_2]$, $[NiCN(H_2O)_5]\cdot Cl_2\cdot 2H_2O$, and $[ZnCN(H_2O)_5]\cdot Cl_2\cdot 4H_2O$, respectively. Infrared data suggests the CN ligand coordinated with the metal ions through the nitrogen lone pair electrons of the C=N group. The TEM images demonstrate the complexes had a uniform, well-structured morphology. We will continue investigating cinchonine's complex interactions with different metal ions. This work aims to deepen our understanding of cinchonine's chelation and ability to form stable complexes, which is compelling and thought-provoking. By studying these interactions in more

detail, we hope to uncover new insights that could lead to innovative applications in fields like catalysis, environmental remediation, and biomedical sciences.

ACKNOWLEDGEMENT

The authors extend their appreciation to Taif University, Saudi Arabia, for supporting this work through project number (TU-DSPP-2024-6).

Funding

This research was funded by Taif University, Saudi Arabia, Project No. (TU-DSPP-2024-6).

REFERENCES

1. Almehizia, A.A.; Alkahtani, H.M.; Zen, A.A.; Obaidullah, A.J.; Naglah, A.M.; Alzughaibi, M.M.; Eldaroti, H.H. Complexes of the antibiotic drug succinylsulfathiazole with the La(III), Sm(III), and Tb(III) ions: Spectral characterizations, microscopic pictures, and thermal properties. *Bull. Chem. Soc. Ethiop.* **2025**, 39, 327-339.
2. Alsawat, M.; Adam, A.M.A.; Refat, M.S.; Alsuhaibani, A.M.; El-Sayed, M.Y. Structural, spectroscopic, and morphological characterizations of metal-based complexes derived from the reaction of 1-phenyl-2-thiourea with Sr^{2+}, Ba^{2+}, Cr^{3+}, and Fe^{3+} ions. *Bull. Chem. Soc. Ethiop.* **2024**, 38, 1803-1814.
3. Adam, A.M.A.; Refat, M.S.; Alsuhaibani, A.M.; El-Sayed, M.Y. Preparation and characterizations of metal-based complexes derived from the reaction of Trizma base with Mg(II), Ca(II), and Ba(II) ions. *Bull. Chem. Soc. Ethiop.* **2024**, 38, 1791-1801.
4. El-Habeeb, A.A.; Refat, M.S. Synthesis, spectroscopic characterizations and biological studies on gold(III), ruthenium(III) and iridium(III) complexes of trimethoprim antibiotic drug. *Bull. Chem. Soc. Ethiop.* **2024**, 38, 701-714.
5. Alsuhaibani, A.M.; Adam, A.M.A.; Refat, M.S.; Kobeasy, M.I.; Bakare, S.B.; Bushara, E.S. Spectroscopic, thermal, and anticancer investigations of new cobalt(II) and nickel(II) triazine complexes. *Bull. Chem. Soc. Ethiop.* **2023**, 37, 1151-1162.
6. Eichhorn, G.L.; Marzilli, L.G. *Advances in Inorganic Biochemistry Models in Inorganic Chemistry*, PTR Prentice-Hall, Inc.: New Jersey; **1994**.
7. Hughes, M.N. *The Inorganic Chemistry of Biological Processes*, 2nd ed., Wiley: Chichester [England]; **1984**.
8. El-Bindary, M.A.; Fathy, A.M. Azo naringenin-based copper(II) complex as DNA binder: Synthesis, spectroscopic characterization, and diverse biological potentials. *Appl. Organomet. Chem.* **2024**, 38, e7460.
9. Amri, N.; Alaghaz, A.M.A.; Bedowr, N.S.; El-Bindary, A.A. Synthesis, structural characterization, in vitro biological activity, and DFT calculations of Cu(II) complex. *Appl. Organomet. Chem.* **2024**, 38, e7551
10. Mojos, K.D.; Orvig, C. Metallodrugs in medicinal inorganic chemistry. *Chem. Rev.* **2014**, 114, 4540-4563.
11. Alessio, E. *Bioinorganic Medicinal Chemistry*, Wiley-VCH Verlag GmbH and Co. KGaA; Germany; **2011**.
12. Younes, A.A.O.; Refat, M.S.; Saad, H.A.; Adam, A.M.A.; Alzoghibi, O.M.; Alsulaim, G.M.; Alsuhaibani, A.M. Complexation of some alkaline earth metals with bidentate uracil ligand: Synthesis, spectroscopic and antimicrobial analysis. *Bull. Chem. Soc. Ethiop.* **2023**, 37, 945-957.

13. Alkathiri, A.A.; Atta, A.A.; Refat, M.S.; Altalhi, T.A.; Shakya, S.; Alsawat, M.; Adam, A.M.A.; Mersal, G.A.M.; Hassanien, A.M. Preparation, spectroscopic, cyclic voltammetry and DFT/TD-DFT studies on fluorescein charge transfer complex for photonic applications. *Bull. Chem. Soc. Ethiop.* **2023**, 37, 515-532.
14. Adam, A.M.A.; Refat, M.S.; Gaber, A.; Grabchev, I. Complexation of alkaline earth metals Mg^{2+}, Ca^{2+}, Sr^{2+} and Ba^{2+} with adrenaline hormone: Synthesis, spectroscopic and antimicrobial analysis. *Bull. Chem. Soc. Ethiop.* **2023**, 37, 357-372.
15. Al-Hazmi, G.H.; Adam, A.M.A.; El-Desouky, M.G.; El-Bindary, A.A.; Alsuhaibani, A.M.; Refat, M.S. Efficient adsorption of Rhodamine B using a composite of Fe3O4@zif-8: Synthesis, characterization, modeling analysis, statistical physics and mechanism of interaction. *Bull. Chem. Soc. Ethiop.* **2023**, 37, 211-229.
16. Alsuhaibani, A.M.; Adam, A.M.A.; Refat, M.S. Four new tin(II), uranyl(II), vanadyl(II), and zirconyl(II) alloxan biomolecule complexes: Synthesis, spectroscopic and thermal characterizations. *Bull. Chem. Soc. Ethiop.* **2022**, 36, 373-385.
17. Al-Hazmi, G.H.; Alibrahim, K.A.; Refat, M.S.; Ibrahim, O.B.; Adam, A.M.A.; Shakya, S. A new simple route for synthesis of cadmium(II), zinc(II), cobalt(II), and manganese(II) carbonates using urea as a cheap precursor and theoretical investigation. *Bull. Chem. Soc. Ethiop.* **2022**, 36, 363-372.
18. Alsuhaibani, A.M.; Refat, M.S.; Adam, A.M.A.; Kobeasy, M.I.; Kumar, D.N.; Shakya, S. Synthesis, spectroscopic characterizations and DFT studies on the metal complexes of azathioprine immunosuppressive drug. *Bull. Chem. Soc. Ethiop.* **2022**, 36, 73-84.
19. El-Sayed, M.Y.; Refat, M.S.; Altalhi, T.; Eldaroti, H.H.; Alam, K. Preparation, spectroscopic, thermal and molecular docking studies of covid-19 protease on the manganese(II), iron(III), chromium(III) and cobalt(II) creatinine complexes. *Bull. Chem. Soc. Ethiop.* **2021**, 35, 399-412.
20. Alosaimi, A.M.; Saad, H.A.; Al-Hazmi, G.H.; Refat, M.S. In situ acetonitrile/water mixed solvents: An ecofriendly synthesis and structure Explanations of Cu(II), Co(II), and Ni(II) complexes of thioxoimidazolidine. *Bull. Chem. Soc. Ethiop.* **2021**, 35, 351-364.
21. Refat, M.S.; Altalhi, T.A.; Al-Hazmi, G.H.; Al-Humaidi, J.Y. Synthesis, characterization, thermal analysis and biological study of new thiophene derivative containing o-aminobenzoic acid ligand and its Mn(II), Cu(II) and Co(II) metal complexes. *Bull. Chem. Soc. Ethiop.* 2021, 35, 129-140.
22. Adehin, A.; Igbinoba, S.I.; Soyinka, J.O.; Onyeji, C.O.; Babalola, C.P.; Bolaji, O.O. Pharmacokinetic parameters of quinine in healthy subjects and in patients with uncomplicated malaria in Nigeria: Analysis of data using a population approach. *CTR* **2019**, 91, 33-38.
23. Boratyński, P.J.; Zielińska-Błajet, M.; Skarżewski, J. Chapter Two - *Cinchona* Alkaloids—Derivatives and Applications. *Alkaloids Chem. Biol.* **2019**, 82, 29-145.
24. Jones, R.A.; Panda, S.S.; Hall, C.D. Quinine conjugates and quinine analogues as potential antimalarial agents. *Eur. J. Med. Chem.* **2015**, 97, 335-355.
25. Adam, A.M.A.; Saad, H.A.; Refat, M.S.; Hegab, M.S.; Al-Hazmi, G.H.; Alsuhaibani, A.M.; Mohamed, H.M. The derivation and characterization of quinine charge-transfer complexes with inorganic and organic acceptors in liquid and solid form. *J. Mol. Liq.* **2022**, 359, 119206.
26. Adam, A.M.A. Nano-structured complexes of reserpine and quinidine drugs with chloranilic acid based on intermolecular H-bond: Spectral and surface morphology studies. *Spectrochim. Acta A* **2014**, 127, 107-114.
27. Eldaroti, H.H.; Gadir, S.A.; Refat, M.S.; Adam, A.M.A. Charge-transfer interaction of drug quinidine with quinol, picric acid and DDQ: Spectroscopic characterization and biological activity studies towards understanding the drug–receptor mechanism. *J. Pharm. Anal.* **2014**, 4, 81-95.
28. Adam, A.M.A.; Eldaroti, H.H.; Hegab, M.S.; Refat, M.S.; Saad. H.A. Measurements and correlations in solution-state for charge transfer products caused from the 1:2 complexation

of TCNE acceptor with several important drugs: Part Two. *Spectrochim. Acta A* **2019**, 211, 166-177.
29. Bellamy, L.J. *The infrared Spectra of Complex Molecules*, Chapman & Hall: London; **1975**.
30. Deacon, G.B.; Phillips, R.J. Relationships between the carbon-oxygen stretching frequencies of carboxylato complexes and the type of carboxylate coordination. *Coord. Chem. Rev.* **1980**, 33, 227-250.